Electronic Supplementary Material (ESI) for Inorganic Chemistry Frontiers.

Supporting Information

Synthesis, Structural, and Electronic Properties of $Sr_{1-x}Ca_xPdAs$

Benjamin W. Y. Redemann,[a] Michael R. Scudder,[a] Daniel Weber,[a] Yaxian Wang,[b] Wolfgang Windl,[b] and Joshua E. Goldberger [a]*

[a]Department of Chemistry and Biochemistry, The Ohio State University, Columbus, Ohio 43210, United States

[b] Department of Materials Science and Engineering, The Ohio State University, Columbus, Ohio 43210, United States

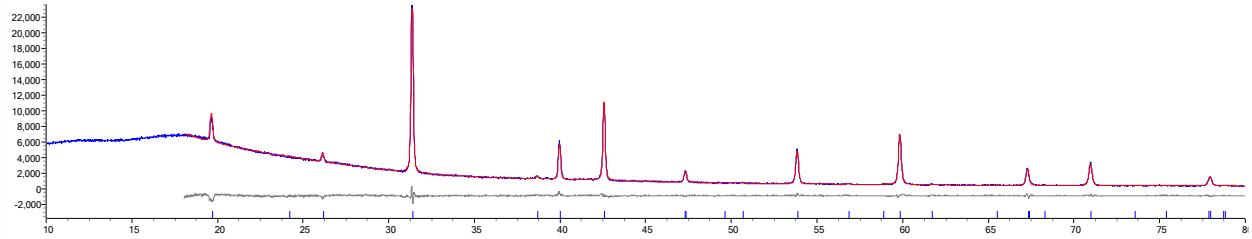

Figure S1. Powder XRD Rietveld refinement results for SrPdAs using TOPAS 6.

Table S1. Crystal data and refinement results for SrPdAs

Empirical Formula	SrPdAs
Fw (g/mol)	268.96
Space group	$P6_3/mmc$
a (Å)	4.2419(10)
c (Å)	9.0103(2)
V (Å$_3$)	140.407(8)
Z	2
T (K)	295
λ (Å)	1.5406
Pattern range (2θ,°)	10-80
R_{wp}	0.0367
R_p	0.0275
R_{exp}	0.0238

Table S2. Fractional atomic coordinates and isotropic displacement parameters based on the refined SrPdAs structure.

Element	x	y	z	Occupancy	B_{eq}
Sr	0	0	0	1	0.52(7)
Pd	0.3333	0.6667	0.25	1	2.84(11)
As	0.6667	0.3333	0.25	1	1.96(12)

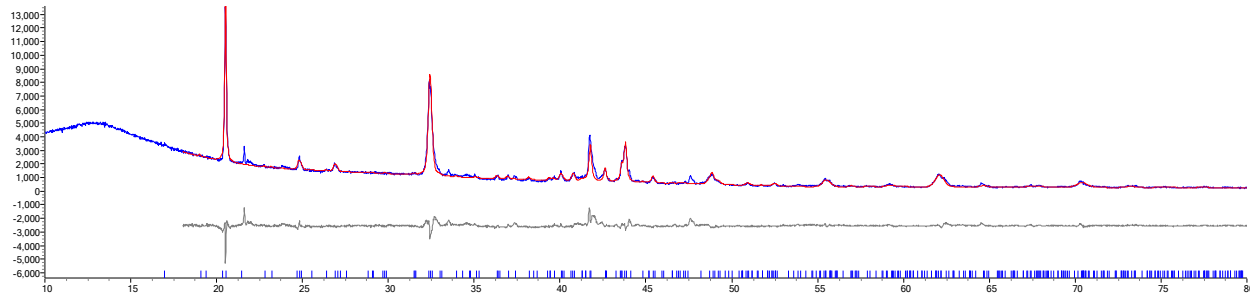

Figure S2. Powder XRD Rietveld refinement results for CaPdAs using TOPAS 6.

Table S3. Crystal data and refinement results for CaPdAs

Empirical Formula	CaPdAs
Fw (g/mol)	221.42
Space group	Pnma
a (Å)	7.136(2)
b (Å)	8.640(3)
c (Å)	16.590(5)
V (Å$_3$)	1022.8(6)
Z	16
T (K)	295
λ (Å)	1.5406
Pattern range (2θ,°)	10-80
R_{wp}	0.0946
R_p	0.0660
R_{exp}	0.0321

Table S4. Fractional atomic coordinates and isotropic displacement parameters based on the refined CaPdAs structure.

Element	x	y	z	Occupancy	B_{eq}
Ca (1)	0.771(5)	0.008(5)	0.183(3)	1	0.6(2)
Ca (2)	0.238(4)	0.011(5)	0.068(3)	1	0.6(2)
Pd (1)	0.6059(3)	¼	0.0346(1)	1	0.8(2)
Pd (2)	0.1022(3)	¼	0.1917(1)	1	0.8(2)
Pd (3)	0.5194(2)	¼	0.5676(1)	1	0.8(2)
Pd (4)	0.1057(3)	¼	0.6651(1)	1	0.8(2)
As (1)	0.451(3)	¼	0.1832(2)	1	0.4(3)
As (2)	0.860(3)	¼	0.5650(2)	1	0.4(3)
As (3)	0.925(4)	¼	0.0602(2)	1	0.4(3)
As (4)	0.427(4)	¼	0.7123(1)	1	0.4(3)

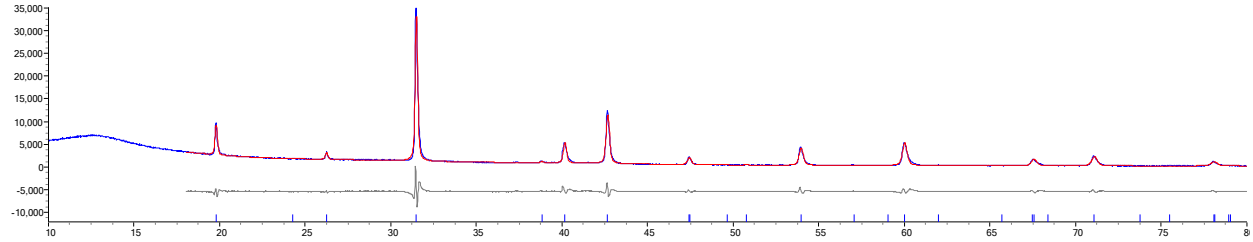

Figure S3. Powder XRD Rietveld refinement results for $Sr_{5/6}Ca_{1/6}PdAs$ using TOPAS 6.

Table S5. Crystal data and refinement results for $Sr_{5/6}Ca_{1/6}PdAs$

Empirical Formula	$Sr_{5/6}Ca_{1/6}PdAs$
Fw (g/mol)	261.04
Space group	$P6_3/mmc$
a (Å)	4.2381(2)
c (Å)	8.9806(5)
V (Å$_3$)	139.696(18)
Z	2
T (K)	295
λ (Å)	1.5406
Pattern range (2θ,°)	10-80
R_{wp}	0.0947
R_p	0.0655
R_{exp}	0.0285

Table S6. Fractional atomic coordinates and isotropic displacement parameters based on the refined $Sr_{5/6}Ca_{1/6}PdAs$ structure.

Element	x	y	z	Occupancy	B_{eq}
Sr	0	0	0	0.87	1.04(18)
Ca	0	0	0	0.13	1.04(18)
Pd	0.3333	0.6667	0.25	1	2.98(17)
As	0.6667	0.3333	0.25	1	1.0(2)

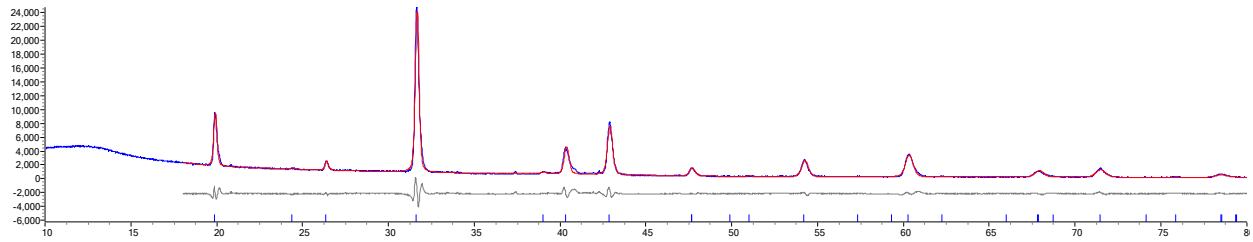

Figure S4. Powder XRD Rietveld refinement results for $Sr_{2/3}Ca_{1/3}PdAs$ using TOPAS 6.

Table S7. Crystal data and refinement results for $Sr_{2/3}Ca_{1/3}PdAs$

Empirical Formula	$Sr_{2/3}Ca_{1/3}PdAs$
Fw (g/mol)	253.12
Space group	$P6_3/mmc$
a (Å)	4.2191(4)
c (Å)	8.9436(8)
V (Å$_3$)	137.87(3)
Z	2
T (K)	295
λ (Å)	1.5406
Pattern range (2θ,°)	10-80
R_{wp}	0.0978
R_p	0.0700
R_{exp}	0.0313

Table S8. Fractional atomic coordinates and isotropic displacement parameters based on the refined $Sr_{2/3}Ca_{1/3}PdAs$ structure.

Element	x	y	z	Occupancy	B_{eq}
Sr	0	0	0	0.69	0.97(19)
Ca	0	0	0	0.31	0.97(19)
Pd	0.3333	0.6667	0.25	1	3.53(15)
As	0.6667	0.3333	0.25	1	2.02(17)

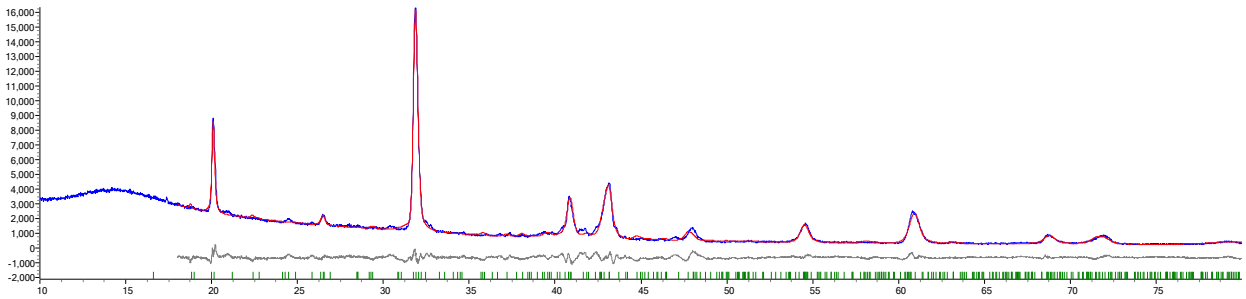

Figure S5. Powder XRD Rietveld refinement results for $Sr_{1/2}Ca_{1/2}PdAs$ using TOPAS 6.

Table S9. Crystal data and refinement results for $Sr_{1/2}Ca_{1/2}PdAs$

Empirical Formula	$Sr_{1/2}Ca_{1/2}PdAs$
Fw (g/mol)	245.19
Space group	Pnma
a (Å)	7.325(2)
b (Å)	8.8231(2)
c (Å)	16.763(4)
V ($Å_3$)	1083.4(5)
Z	8
T (K)	295
λ (Å)	1.5406
Pattern range (2θ,°)	10-80
R_{wp}	0.0833
R_p	0.0597
R_{exp}	0.0299

Table S10. Fractional atomic coordinates and isotropic displacement parameters based on the refined $Sr_{1/2}Ca_{1/2}PdAs$ structure.

Element	x	y	z	Occupancy	B_{eq}
Ca (1)	0.7631(3)	-0.007(4)	0.1893(2)	0.5	1.4(3)
Sr (1)	0.7631(3)	-0.007(4)	0.1893(2)	0.5	1.4(3)
Ca (2)	0.2530(2)	-0.006(4)	0.0674(2)	0.5	1.4(3)
Sr (2)	0.2530(2)	-0.006(4)	0.0674(2)	0.5	1.4(3)
Pd (1)	0.6077(2)	¼	0.0439(1)	1	1.75(18)
Pd (2)	0.1003(3)	¼	0.1870(1)	1	1.75(18)
Pd (3)	0.5358(3)	¼	0.5650(1)	1	1.75(18)
Pd (4)	0.0883(2)	¼	0.6716(1)	1	1.75(18)
As (1)	0.431(3)	¼	0.1872(1)	1	0.3(2)
As (2)	0.8693(3)	¼	0.5609(2)	1	0.3(2)
As (3)	0.933(3)	¼	0.0540(1)	1	0.3(2)
As (4)	0.415(4)	¼	0.6995(1)	1	0.3(2)

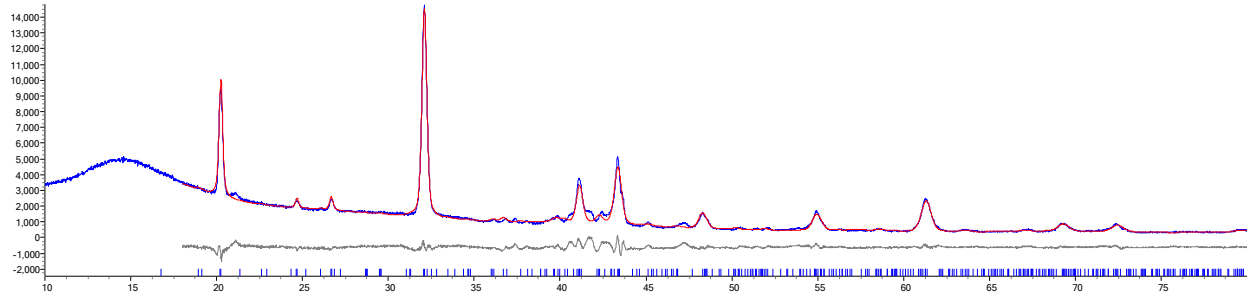

Figure S6. Powder XRD Rietveld refinement results for $Sr_{1/3}Ca_{2/3}PdAs$ using TOPAS 6.

Table S11. Crystal data and refinement results for $Sr_{1/3}Ca_{2/3}PdAs$

Empirical Formula	$Sr_{1/3}Ca_{2/3}PdAs$
Fw (g/mol)	237.27
Space group	Pnma
a (Å)	7.2337(9)
b (Å)	8.7761(4)
c (Å)	16.648(4)
V ($Å_3$)	1056.8(3)
Z	8
T (K)	295
λ (Å)	1.5406
Pattern range (2θ,°)	10-80
R_{wp}	0.0765
R_p	0.0545
R_{exp}	0.0286

Table S12. Fractional atomic coordinates and isotropic displacement parameters based on the refined $Sr_{1/3}Ca_{2/3}PdAs$ structure.

Element	x	y	z	Occupancy	B_{eq}
Ca (1)	0.750(7)	0.002(4)	0.1809(3)	0.65	0.9(5)
Sr (1)	0.750(7)	0.002(4)	0.1809(3)	0.35	0.9(5)
Ca (2)	0.247(4)	0.0106(3)	0.0556(2)	0.65	0.9(5)
Sr (2)	0.247(4)	0.0106(3)	0.0556(2)	0.35	0.9(5)
Pd (1)	0.5997(3)	¼	0.0388(1)	1	2.46(17)
Pd (2)	0.1034(3)	¼	0.1933(1)	1	2.46(17)
Pd (3)	0.5551(2)	¼	0.5724(1)	1	2.46(17)
Pd (4)	0.117(3)	¼	0.6677(1)	1	2.46(17)
As (1)	0.421(4)	¼	0.1902(1)	1	1.1(2)
As (2)	0.8875(3)	¼	0.5701(2)	1	1.1(2)
As (3)	0.9343(3)	¼	0.0622(1)	1	1.1(2)
As (4)	0.430(4)	¼	0.7098(1)	1	1.1(2)

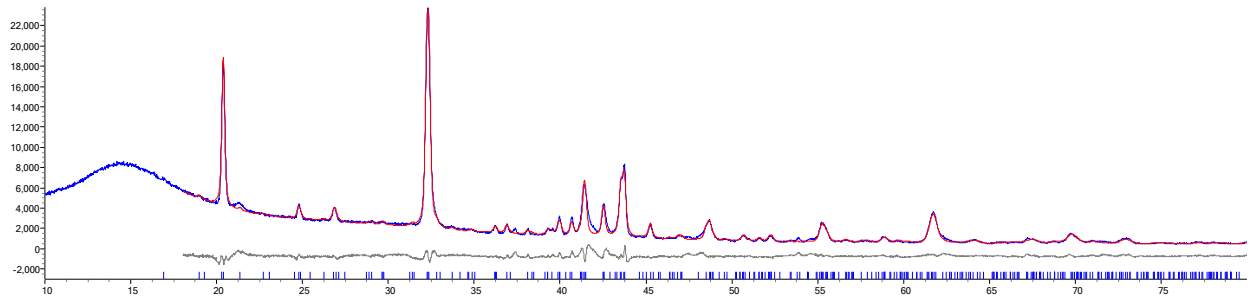

Figure S7. Powder XRD Rietveld refinement results for $Sr_{1/6}Ca_{5/6}PdAs$ using TOPAS 6.

Table S13. Crystal data and refinement results for $Sr_{1/6}Ca_{5/6}PdAs$

Empirical Formula	$Sr_{1/6}Ca_{5/6}PdAs$
Fw (g/mol)	229.34
Space group	Pnma
a (Å)	7.1565(4)
b (Å)	8.7162(5)
c (Å)	16.6324(9)
V (Å$_3$)	1037.48(1)
Z	8
T (K)	295
λ (Å)	1.5406
Pattern range (2θ,°)	10-80
R_{wp}	0.0744
R_p	0.0518
R_{exp}	0.0227

Table S14. Fractional atomic coordinates and isotropic displacement parameters based on the refined $Sr_{1/6}Ca_{5/6}PdAs$ structure.

Element	x	y	z	Occupancy	B_{eq}
Ca (1)	0.7739(2)	0.0050(3)	0.1891(1)	0.83	0.7(4)
Sr (1)	0.7739(2)	0.0050(3)	0.1891(1)	0.17	0.7(4)
Ca (2)	0.2580(2)	0.0197(2)	0.0666(1)	0.83	0.7(4)
Sr (2)	0.2580(2)	0.0197(2)	0.0666(1)	0.17	0.7(4)
Pd (1)	0.5969(2)	¼	0.0340(6)	1	1.40(7)
Pd (2)	0.1140(2)	¼	0.1961(9)	1	1.40(7)
Pd (3)	0.5143(2)	¼	0.5667(1)	1	1.40(7)
Pd (4)	0.1121(2)	¼	0.6718(1)	1	1.40(7)
As (1)	0.4571(2)	¼	0.1835(9)	1	0.83(12)
As (2)	0.8750(2)	¼	0.5697(2)	1	0.83(12)
As (3)	0.9326(2)	¼	0.0616(1)	1	0.83(12)
As (4)	0.4300(3)	¼	0.7149(9)	1	0.83(12)

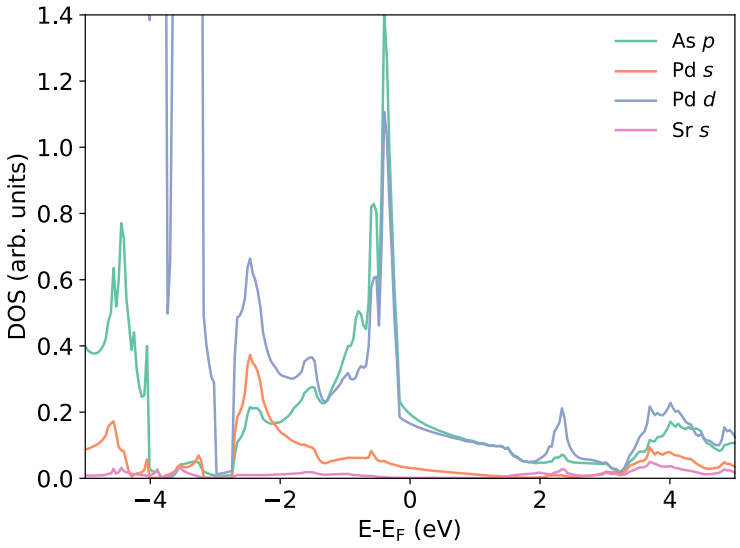

Figure S8. Density of states of SrPdAs calculated by DFT.

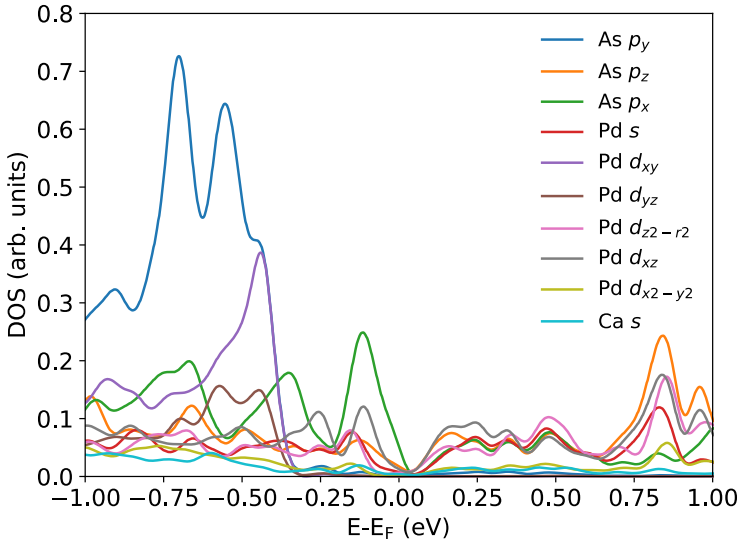

Figure S9. Density of states of CaPdAs calculated by DFT.

Phase Stability Evaluation from the DFT-Calculated Convex Hull

The thermodynamic stability in a chemical system can be assessed by a comparison of the free energies of the different phases present. For a solid system in ambient conditions, the external pressure has a negligible effect on the free energy. Thus, in the low-temperature limit where the entropy terms approach zero, the relevant thermodynamic potential is the total energy of the system as calculated by DFT.

Within the convex-hull approach[1] for a two-component system, one first calculates the energies of all (relevant) phases that the two components can form. For the phase whose stability we examine here, Sr_2PdAs_2 we examine the phases formed by the two components A = Pd and B = SrAs, which encompass SrPdAs and Sr_2PdAs_2 besides the pure-component phases. For the convex hull, all energies are first normalized per atom, i.e., $\bar{E}(x_A, x_B) = \frac{E(A_nB_m)}{n+m}$ with $x_A = n/(n+m)$ and $x_B = m/(n+m)$. From these, formation energies with respect to the endpoints for all phases are calculated, i.e., $\bar{E}_f(x_A, x_B) = \bar{E}(x_A, x_B) - x_A\bar{E}(x_A = 1, x_B = 0) - x_B\bar{E}(x_A = 0, x_B = 1)$ and plotted versus composition. The line connecting the end points through the lowest-energy points such that no other point is below the line is called the convex hull. Phases above the convex hull are unstable and will transform to the phase on the hull with the same composition in case there is one, or otherwise decompose into the two phases at the end of the tie line under it. Figure S10 shows the convex hull plot of the Pd-SrAs system. The Sr_2PdAs_2 phase is 163 meV/atom above the convex hull and thus unstable with respect to decomposition into SrAs and SrPdAs.

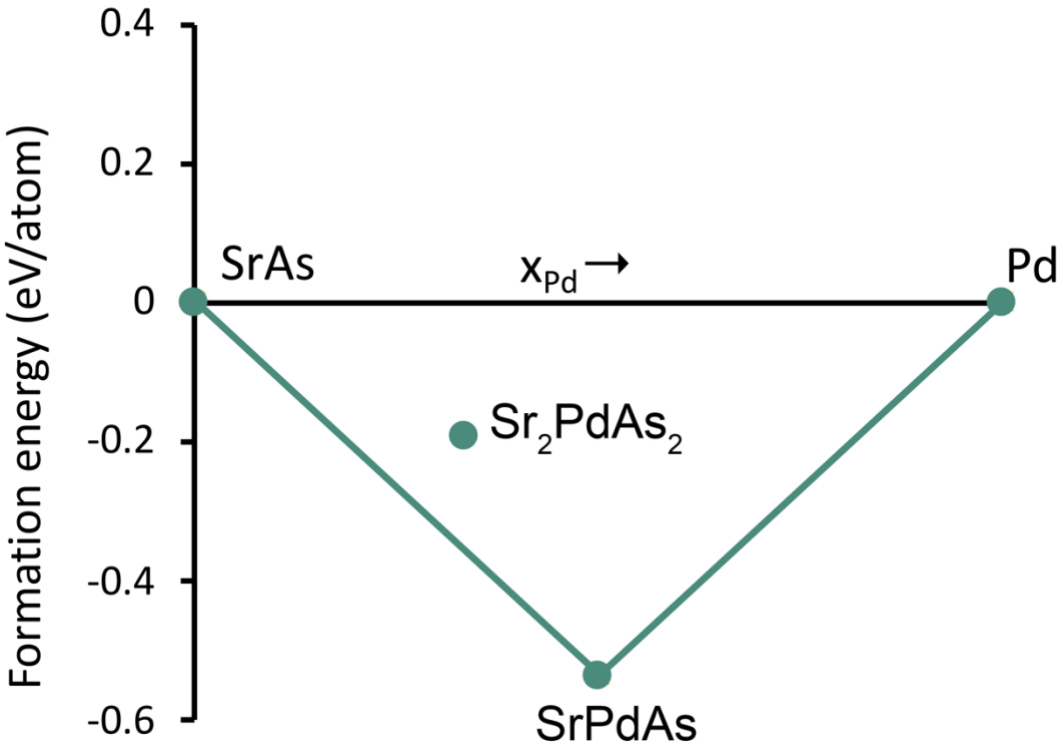

Figure S10. DFT results for the convex hull of the SrAs-Pd system.

References

1. G. Hautier, in *Prediction and Calculation of Crystal Structures: Methods and Applications*, eds. S. Atahan-Evrenk and A. Aspuru-Guzik, Springer International Publishing, Cham, 2014, Data Mining Approaches to High-Throughput Crystal Structure and Compound Prediction, pp. 139-179.